SYNTHESIS AND CHARACTERISATION OF GRAPHENE OXIDE AND ITS NANOCOMPOSITE FOR BIOSENSING APPLICATIONS

A Major Project Report Submitted in partial fulfillment for the Award of the Degree of

MASTER OF TECHNOLOGY

IN

POLYMER TECHNOLOGY

Submitted by

SARTHAK SINGH

2K15/PTE/09

UNDER THE ESTEEMED GUIDANCE OF

PROF. D. KUMAR

Department of Applied Chemistry & Polymer Technology

Delhi Technological University, Delhi-110042

July 2017

CERTIFICATE

This is to certify that the project report entitled "**SYNTHESIS AND CHARACTERISATION OF GRAPHENE OXIDE AND ITS NANOCOMPOSITE FOR BIOSENSING APPLICATIONS"** submitted by **Sarthak Singh (2K15/PTE/09)** in partial fulfillment for the award of degree of Master of Technology in Polymer Technology to Delhi Technological University, Delhi, is a record of the work carried out by him under our supervision. The project embodies the original work by him to the best of our knowledge and has not been submitted to any other degree of this or any other university. The matter embodied in this project report is original and not copied from any source without proper citation.

Prof. D. Kumar
Professor
Department of Applied Chemistry
& Polymer Technology
Delhi Technological University
New Delhi -110042

Dr. Archana Rani
Head of the department
Department of Applied Chemistry
& Polymer Technology
Delhi Technological University
New Delhi -110042

DECLARATION

I **Sarthak Singh** hereby declare that the thesis entitled "**Synthesis And Characterisation Of Graphene Oxide And Its Nanocomposite For Biosensing Applications"** is an authentic record of research work done by me under the supervision of **Prof. D. Kumar,** Professor, Delhi Technological University. This work has not been previously submitted for the award of any degree or diploma of this or any other University/Institute.

Dated Sarthak Singh

ACKNOWLEDGEMENT

It gives me immense pleasure to express my deepest sense of gratitude and sincere thanks to highly respected and esteemed guide **Prof. D. Kumar**, for his valuable guidance, encouragement and help for completing this work. His useful suggestions for this whole work and co-operative behavior are sincerely acknowledged.

I also wish to express my gratitude to Dr. Archana Rani, HOD (Department of Applied Chemistry & Polymer Technology) for her kind hearted support. I am also grateful to all teachers for their constant support and guidance.

I'm grateful to Dr. C.M. Pandey for his invaluable guidance, support and motivation in my research work.

I also wish to express my indebtedness to my parents as well as my family members whose blessings and support always helped me to face the challenges ahead.

At the end I would like to express my sincere thanks to all my friends and others who helped me directly or indirectly during this project work.

Sarthak Singh

LIST OF FIGURES

LIST OF TABLES

Chapter No.	CONTENT	Page No.
	Abstract	1
1.	Introduction	2
2.	Literature Review	5
3.	Materials and Methods	11
4.	Results and Discussion	18
5.	Conclusions	37
	References	38

ABSTRACT

Graphene Oxide (GO) and Titanium dioxide (TiO_2) nanocomposites have been synthesized by chemical oxidation meathod. The materials were characterized using Fourier transform infrared spectroscopy, powder X-ray diffraction, scanning electron microscopy, differential scanning calorimetry. The synthesized GO-TiO_2 nanocomposites were used to prepare film onto indium tin oxide coated glass substrate by electrophoretic deposition at different potentials. The cyclic voltammetry analysis of the film are conducted at different scan rates (10 to 300 mVs^{-1}) shows that the anodic peak current increases as the scan rate is increased. Through CV studies we observed that there is an increase in value of average surface coverage and diffusion coefficient in case of GO-TiO_2 /ITO electrode film as compared to GO/ITO electrode. The electrochemical sensing studies of hydrogen peroxide (H_2O_2) shows increase in anodic peak current with increase in H_2O_2 concentration(50 to 200 μM) in PBS (pH 7.4) containing 5 mM $[Fe(CN)_6]^{3-/4-}$.

CHAPTER 1

INTRODUCTION

Graphene has been considered as “the thinnest material in our universe” [1], and has drawn an enormous amount of attention as it shows many interesting properties. Graphene is a single layer of carbon atoms with hexagonal arrangement in a two-dimensional lattice which is the core building block for graphitic materials. The unique properties of graphene include fast electron transportation, high thermal conductivity, excellent mechanical stiffness and good biocompatibility [2]. These properties result in promising applications in [3], field-effect transistors [4], electromechanical resonators [5], solar cells [6] and electrochemical sensors [7,8].

The determination of hydrogen peroxide has a great significance in chemistry, biology [9-10], clinical control [11] and environmental protection [12]. There are many techniques which have been utilized to detect hydrogen peroxide, including titrimetry [13], fluorimetry [14], spectrophotometry [15], chemiluminescence [16] and electrochemical sensors [17–19]. Hydrogen peroxide (H_2O_2) has a great importance in pharmaceutical, clinical, environmental, mining, textile and food manufacturing applications [20]. H_2O_2 can also be used as a signalling molecule in regulating diverse biological processes such as immune cell activation, vascular remodelling, apoptosis, stomatal closure and root growth in living organisms [21–23]. Therefore, the study on H_2O_2 detection is of practical significance for both academic and industrial purposes. There are many techniques for determination of hydrogen peroxide (H_2O_2) such as fluorimetry [24], chemiluminescence [25], fluorescence [26] and spectrophotometry [27]. These techniques are complex, costly and time consuming. Electrochemistry may offer easy, fast, responsive, and cost effective means as H_2O_2 is an electroactive molecule [28] in comparison of other conventional techniques [29].

A biosensor device consists of a biological sensing element intimately connected or integrated within a transducer. The fundamental principle of a biosensor is to produce an electronic digital signal is proportional to the concentration of the particular analyte [30]. This emerging field

offers new and powerful tools for the exciting alternative to traditional methods, thereby allowing rapid and multiple detections and the diagnosis of any analyte.

H_2O_2 biosensors are widely made-up by using carbon nanotubes (CNTs) because CNTs have high electrical conductivity and excellent electrocatalytic activity towards H_2O_2. The CNTs have been successfully utilized as "molecular wires" which made to realize the direct electron transfer between redox centers of enzymes and electrodes, that leads to the new mediator-free biosensor [31–33]. Another carbon-based material, i.e. , graphene shows very beneficial characteristics which can be very useful in designing of electrochemical sensors, such as high surface area-to-volume ratio, fast electron transferring rate and good biocompatibility. Due to the convenient and low cost of fabrication, graphene is likely to be an ideal substitute electrode material to carbon nanotubes (CNTs).

1.1 Research Objective

Graphene is an emerging material with unique electrical, thermal and mechanical properties with a wide range of applications. Therefore, for analysis of graphene properties into useful output, it has to be converted into a suitable form like graphene papers, transparent/conducting films, graphene fiber or 3D framework and its nanocomposites. The main objective of this project work is:

- Synthesis of graphene oxide (GO) and its nanocomposite with titanium oxide (TiO_2).
- Characterization of GO and GO-TiO_2 nanocomposite using FTIR, XRD, SEM, UV spectroscopy, differential scanning calorimetry.
- Electrophoretic deposition of GO and GO-TiO_2 nanocomposite film on indium-tin-oxide coated glass substrate (ITO) at optimized condition.
- Electrochemical studies of the deposited film using CV technique.
- Evaluation of hydrogen peroxide sensing performance at different concentrations of H_2O_2.

1.2 Organization of Thesis

Chapter 1: (Introduction) to provide a brief overview of the research background including the definition of the problem.

Chapter 2: (Literature Review) to provide information about carbon and its isotopes, graphene history, synthesis and its properties, film deposition techniques of nano particles, electrochemistry of GO and its nanocomposites.

Chapter 3: (Materials and Methods) to describe about the material and equipment used in the present study followed by the experimental procedure which includes synthesis of graphene oxide along with graphene oxide and titanium dioxide nanocomposite, its film deposition on ITO coated glass **substrate** and details of experimental techniques and parameters.

Chapter 4: (Results and Discussion) in this chapter results of different characterization and their inferences have been discussed.

Chapter 5: (Conclusions) provides major findings in this research work.

CHAPTER 2

LITERATURE REVIEW

Until 1980s, there were only two well known members of carbon family , i.e. , graphite and diamond. A great revolution has come with the discovery of other carbon allotropes, viz. , fullerenes, CNTs and very recently graphene. Among all these carbonaceous material, graphene has attracted tremendous research interest due to its unique, outstanding properties as well as structural features [34]. Graphene has shown a variety of intriguing properties including superior mechanical properties (intrinsic strength of ~130 GPa), complete impermeability to any gases, ability to sustain extremely high densities of electric current (a million times higher than copper), high electron mobility at room temperature (250,000 cm^2/Vs), exceptional thermal conductivity (5000 $Wm^{-1}K^{-1}$) and easy chemical functionalization comparative to other materials (Table-1) [35-36]. Moreover, the cost of production of graphene is very low as compared to other carbon-based nanomaterials.

Table1: Properties of graphene, CNT, nano sized steel and polymers

Materials	Tensile strength (GPa)	Thermalconductivity (W/mK)	Electrical conductivity (S/m)
Graphene	160±10	$(4.84\pm0.44)\times10^3$ to $(5.30\pm0.48)\times10^3$	7200
CNT	60-150	3500	3000-4000
Nano sized steel	1769	5-6	1.35×10^6
Plastic (HDPE)	0.018-0.020	0.46-0.52	Insulator
Rubber (Natural)	0.02-0.03	0.13-0.142	Insulator
Fiber (Natural)	3.62	0.04	Insulator

The different molecular architecture is responsible for the wide difference in their properties, despite having a similar carbon-carbon network as other carbon materials. Therefore, a brief introduction of carbon and its allotropes is essential for better understanding of graphene.

2.1 BACKGROUND OF CARBON MATERIALS

Initially, carbon was discovered by A.L. Lavoisier as charcoal in 1789. It is widely distributed in nature with coal as its main source. Carbon has 4 electrons in four hybridized bonding orbital ($2s^1 2px^1 2py^1 2pz^1$) that are available to form covalent bonds. It is being developed into different allotropes, viz. , diamond, graphite, fullerenes, carbon nanotubes and more lately graphene. These allotropes show a variety of interesting electronic and structural properties due to the coexistence of sp^2 and sp^3 hybridized carbon atoms in different proportions.

2.2 GRAPHITE

Graphite is a soft material in which carbon atoms are bonded trigonally with three carbon atoms in the plane as shown in fig 1 . Due to such type of bonding, we assume a two dimensional layer type architecture has sp^2 hybridization. Due to intermolecular interactions, these layers stack over each other to form 3D graphitic structure. These layers are bonded by weak Vander Walls forces responsible for the softness of graphite and thus show lubricating properties. The delocalization of one of the other electrons of each atom forms a π-cloud due to which graphite is an electrical conductor. The interlayer distance between layers is found to be 3.34Å, with ABAB…. stacking sequence..

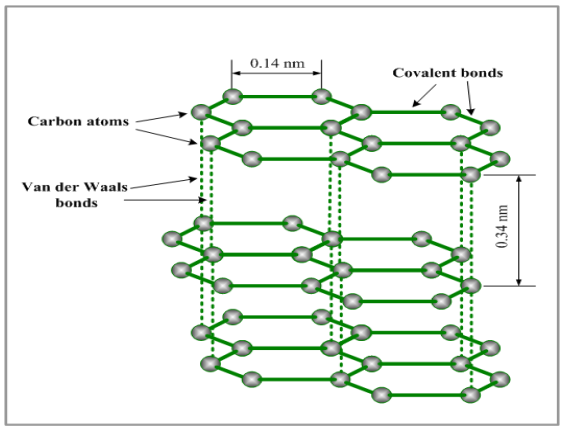

Fig 1: General structure of graphite

2.3 DIAMOND

Diamond is an allotrope of carbon with sp^3 hybridized orbitals which are arranged in 3D space to form tetrahedral structure as shown in fig 2. Diamond is the hardest known material due to strong covalent bonding. All the orbitals in diamond are filled with no free electron in valence shell due to which diamond is an insulating material with wide band gap. Most of the applications of diamond are related to industrial purpose like grinding, drilling, polishing and cutting due to its unparallel hardness [37]. Besides its suitable refractive index, high optical dispersion and ability to cut along various crystal planes give the diamond its characteristic luster which makes it precious gemstone for jewellery and adornments.

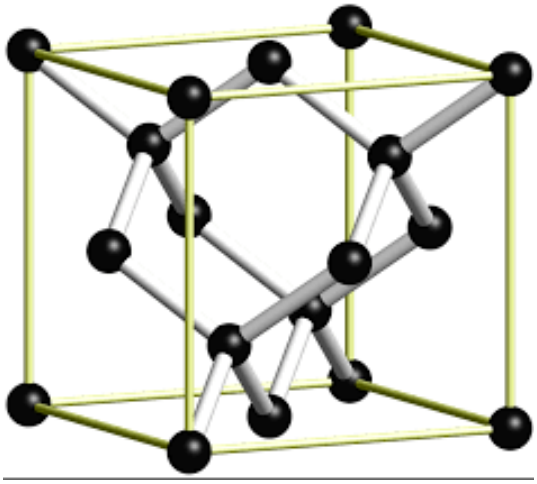

Fig 2: General structure of diamond

2.4 FULLERENE

A fullerene is an allotrope of carbon which has many forms such as hollow sphere, tube and many other shapes. Spherical fullerenes, also referred to as Buckminsterfullerenes or buckyballs. Fullerenes are similar to graphite is made of stacked graphene sheets of linked hexagonal ring, but they may also have either pentagonal or heptagonal rings as shown in fig 3. Buckyballs are subject to intense research, both for their unique chemistry and for their technological applications, especially in nanotechnology, electronics and material science, e.g. , as electron

acceptor on photovoltaic, for making inclusion compounds, quantum mechanics studies, superconductivity and anti-tumor research [38].

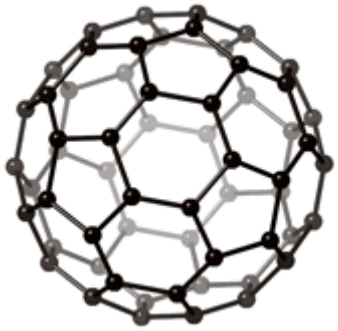

Fig 3: General structure of fullerene

2.5 CARBON NANOTUBES

Carbon nanotubes (CNTs) are allotropes of carbon which have cylindrical nanostructure as shown in fig 4. CNTs are constructed with length-to-diameter ratio of up to 135,000,000:1, considerably larger as compared to any other material. Due to their, surprising mechanical, electrical and thermal properties, carbon nanotubes are used as additives to various structural resources. For example, CNTs are used to manfacture petite portions of the material(s) in some (primarily carbon fiber) golf clubs, bats or automobile parts.. The graphene sheets are rolled at specific and discrete angles, and the combination of the rolling angle and radius decides the nanotube properties; for example, whether the individual nanotube shell is a metal or semiconductor. CNTs are differentiated as single-walled nanotubes (SWNTs) and multi-walled nanotubes (MWNTs). Individual nanotubes naturally align themselves into "ropes" which are held together by Van der Waals forces, more specifically, π-stacking.

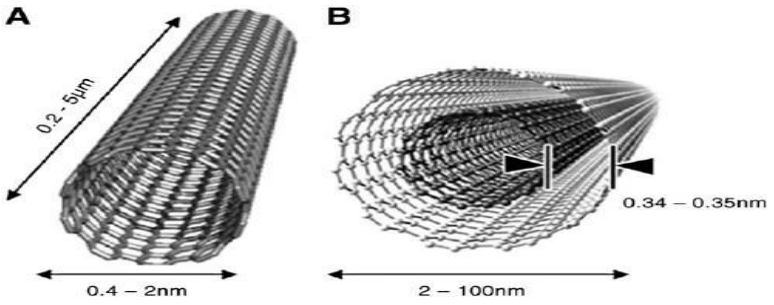

Fig 4: Structure of (a) single walled and (b) multi walled CNT

2.4 GRAPHENE

The term graphene first appeared in 1987 to describe single sheets of graphite as one of the constituent of graphite intercalation compounds (GIC). Conceptually, a GIC is a crystalline salt of the intercalant and graphene. The term was also used in early descriptions of carbon nanotubes as well as for epitaxial graphene.

Graphene is a one-atom-thick planar sheet of sp^2 bonded carbon atoms which are densely packed in a honeycomb shaped lattice. In a 2-D carbon system for graphene, three carbon electrons from four hybridized bonding electrons form strong in-plane sp^2 bonds consisting of the honeycomb structure, and a fourth electron spreads out over the top or bottom of the layer as a π electron.

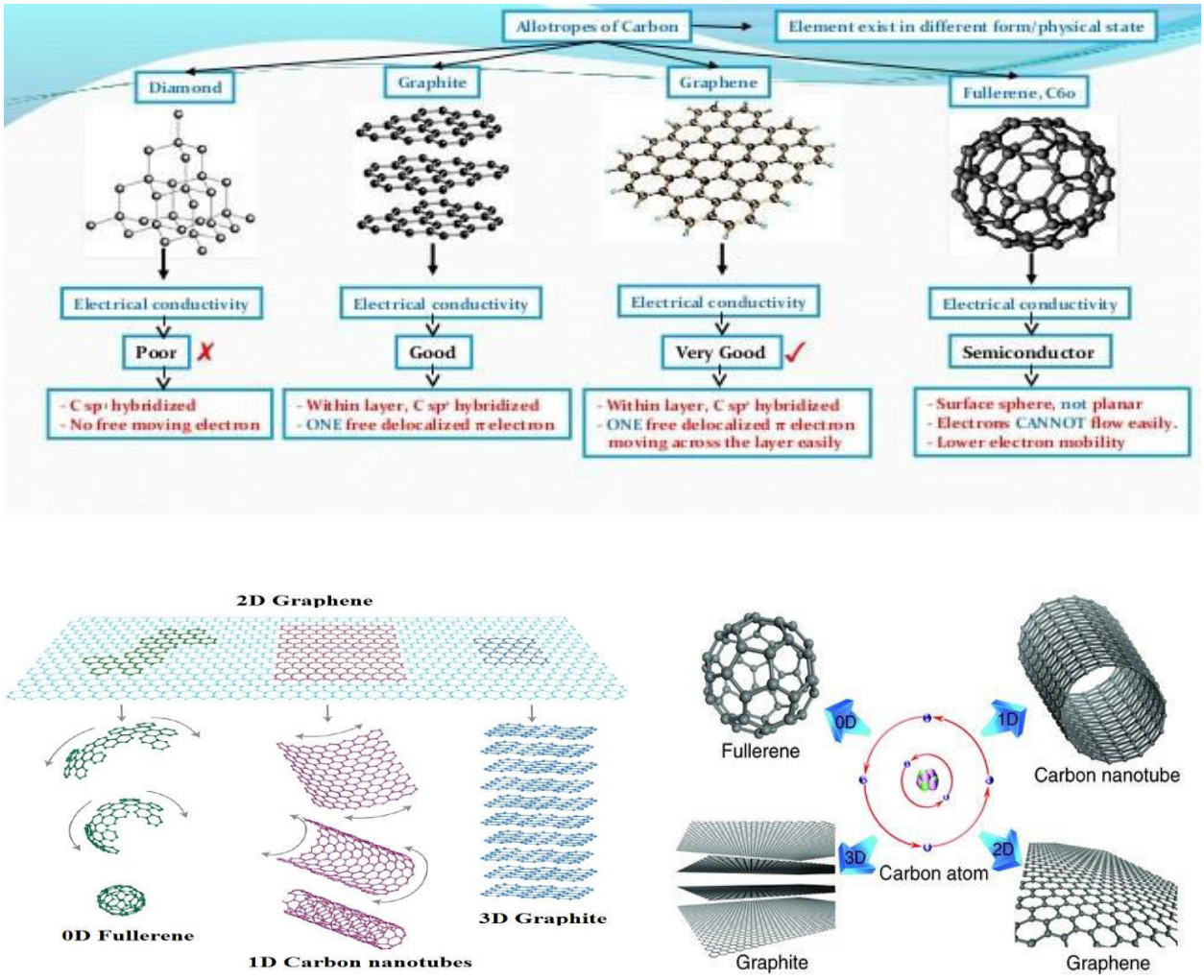

Fig 5: Graphene and its relation to fullerene, CNT and graphite

2.6 OVERVIEW OF GRAPHITIC OXIDE

Graphene oxide, also known as graphitic oxide or graphitic acid, is a compound made up of carbon, oxygen and hydrogen atoms in changeable ratios, which is synthesized by treating graphite with strong oxidizers. The maximun yield product is of yellow colour with C/O ratio between 2.1 to 2.9 which has a much larger and irregular spacing as compared structure of graphite.

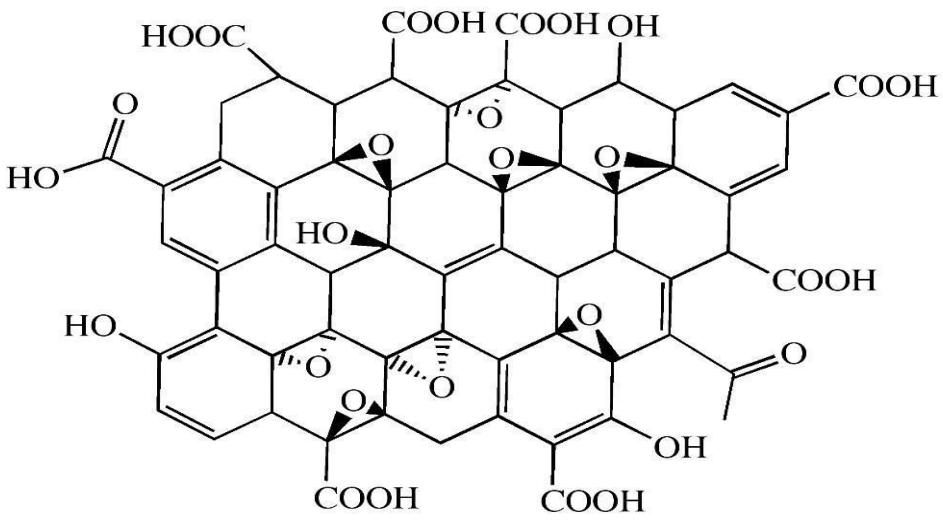

Fig 6: General structure of Graphitic Oxide

CHAPTER 3

MATERIALS AND METHODS

3.1 RAW MATERIAL

- Graphite powder (CHD, India)
- Sodium nitrate $NaNO_3$ (Fischer scientific)
- Potassium permanganate $KMnO_4$ (Fischer scientific)
- Sulphuric acid H_2SO_4, 98% (Merck chemicals)
- Hydrogen peroxide H_2O_2, 30% (Speck pure chemicals)
- ITO coated glass
- Distilled water
- PBS (pH 7.4) containing 5 mM $[Fe(CN)_6]^{3-/4-}$ buffer solution
- Titanium dioxide TiO_2, RFCL Limited

3.2 SYNTHESIS OF GO

GO was prepared using modified Hummers method. For this we took a clean, dry beaker and rinsed it using concentrated sulphuric acid. Then 75 ml of H_2SO_4 was added and stirred on a

magnetic stirrer followed by the addition of 3 gm of $NaNO_3$. The solution was stirred for 1 h , after that 3 gm of graphite was added and the resulting solution was further stirred for 3 h. After the stipulated time 9 gm of $KMnO_4$ was slowly added while keeping the solution in an ice bath at temperature below 20 ^oC. The solution was stirred for 24 h and after that 150 ml of water was added to this solution. After 20 min more water (420 ml) was added to the solution and the mixture was stirred for 10 min. Further, H_2O_2 was added to the solution till a bright yellow color was observed. The solution was filtered and washed with water 2-3 times or till all the acid is removed. The solution was centrifuged and the GO pulp was removed and was put in oven for 5-6 h. The powder was collected in eppendorf.

3.3 SYNTHESIS OF GO-TIO_2 NANOCOMPOSITE

For the synthesis of GO-TiO_2 nanocomposite, concentrated sulphuric acid (75 ml) $NaNO_3$ (3 gm) was added in a beaker under stirring. After 1 h, 3 gm of graphite was added the solution was stirred for 3 h followed by the addition of 9 gm of $KMnO_4$ (very slowly) along with 3 gm of TiO_2 while keeping the solution in an ice bath at temperature below 20 ^oC. The solution was stirred for 24 h and after that 150 ml of water was added to this solution. After 20 min of stirring more water was added (420 ml) to the solution. Further, H_2O_2 was poured to the solution till a yellow green color is obtained. The solution was filtered washed the precipitate with water 2-3 times or till all the acid is removed. Centrifuged the solution and the pulp is removed. The solution was centrifuged and the GO pulp was removed and was put in oven for 5-6 h. The powder was collected in eppendorf.

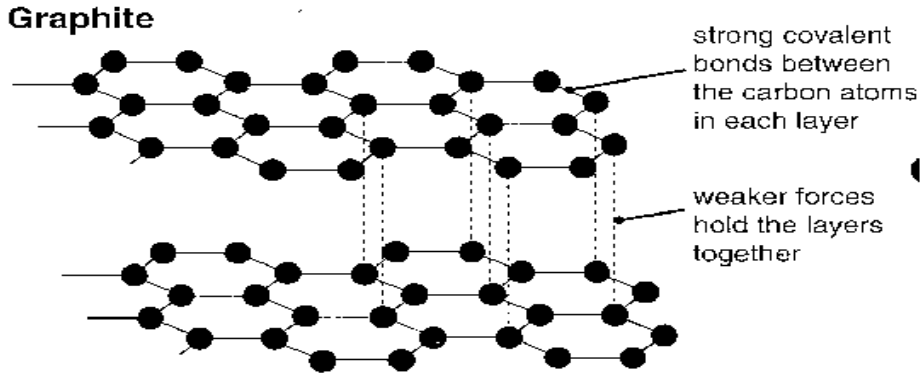

OXIDATION OF GRAPHITE

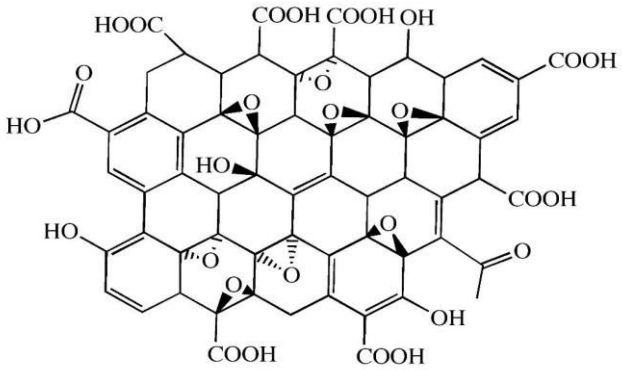

Fig 7: Scheme showing the Oxidation of Graphite

(a).

(b)

(c).

(d).

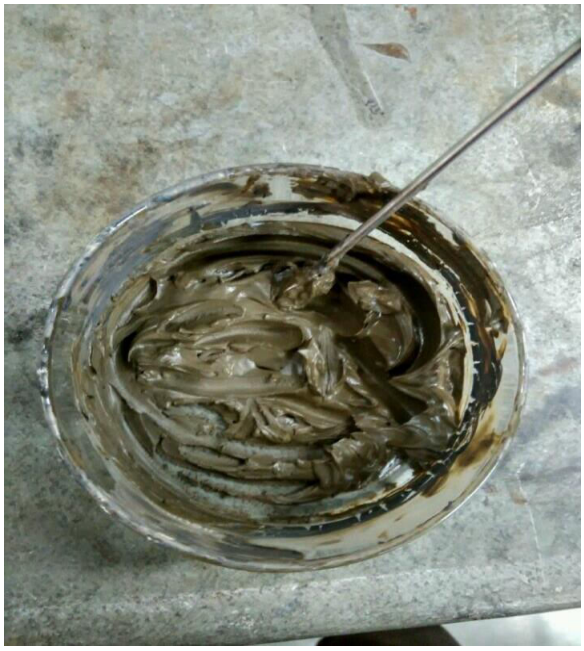

(e).

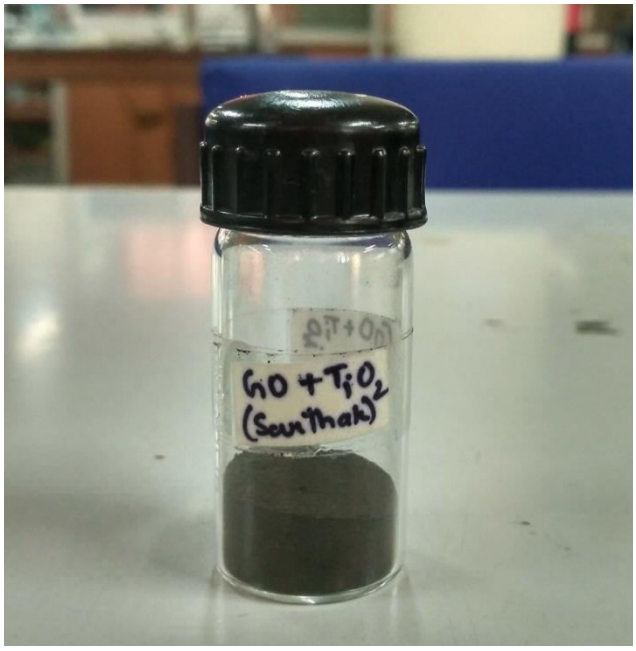

(f).

Fig 8: Different phases of synthesis of GO-TiO_2 nanocomposite (a)&(b) solution on the magnetic stirrer after adding graphite (c) solution on ice bath (d) pulp after centrifuge (e) nanocomposite pulp after 5 hrs in oven (f) GO-TiO_2 nanocomposite in powdered form

3.3 ELECTROPHORITIC DEPOSITION OF GO-TiO_2 on ITO COATED GLASS SUBSTRATE

Electrophoretic deposition (EPD) has been known since 1808 when the Russian scientist "Ruess" observed an electric field induced movement of clay particles in water. However, the first practical use of this technique was demonstrated in 1933 when the deposition of thoria particles on a Pt cathode as an emitter for electron tube application was patented in the USA.

EPD is a technique that has a wide range of applications in the processing of advanced ceramic materials and coatings. Recently, it has gained interest both in the industrial sector and academia not only because of its high versatility of its use with different materials and their combinations but also because of the cost-effectiveness.

3.3.1 Electrophoretic deposition

Electrophoretic deposition (EPD) is one of the colloidal processes in ceramic production and has many advantages such as short formation time, needs simple apparatus, little restriction of the shape of the substrate, no requirement for binder burnout as the green coating contains few or no organics.

Compared to other advanced shaping techniques, the EPD process is very versatile since it can be modified easily for a specific application. For example, deposition can be made on flat, cylindrical or any other shaped substrate with only little changes in electrode design and positioning. Despite of being a wet process, EPD offers easy control of the thickness and morphology of a deposited film through simple adjustment of the deposition time and applied potential. The term 'electrodeposition' is often used somewhat ambiguously to refer to either electroplating or electrophoretic deposition, although it more usually refers to the former.

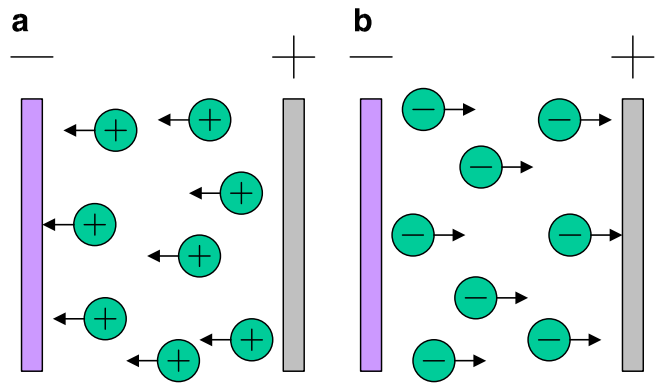

Fig 9: Schematic illustration of the two electrophoretic deposition processes

3.3.2 Factors influencing EPD

- **Parameters related to the suspension**

1. Size of particle
2. Electrical properties of liquid, i.e. , dielectric constant and conductivity
3. Fluid property suspension, i.e. , viscosity
4. Stability of suspension

- **Parameters related to the process**

1. Deposition time
2. Voltage applied
3. Solid concentration in suspension
4. Conductivity of substrate

3.3.3 Electrophoretic deposition of GO-TiO_2 nanocomposite over pre-hydrolyzed ITO electrode

The synthesized GO-TiO_2 nanocomposite was cathodically deposited using EPD technique onto a pre-hydrolyzed ITO electrode using a two-electrode system, with parallel-placed platinum as the reference electrode. Prior to deposition, the colloidal suspension was sonicated in deionized water for 30 min. Magnesium nitrate hexahydrate $Mg(NO_3)_2.6H_2O$ was added into the colloidal solution and sonicated for 10 min. For deposition, 12 mL of the solution was taken out and subjected to EPD at DC potential of 12V for 10 s. The obtained uniform film of GO-TiO_2 nanocomposite was stored in desiccator.

Fig 10: Electrophoretic unit along with EPD cell

CHAPTER 4

RESULTS AND DISCUSSION

4.1 FOURIER TRANSFORM INFRA RED spectroscopy

The FTIR spectra have been used to measure, how well the sample absorbs the light at which wavelength, by using this we can find out, which functional group is present in the material.

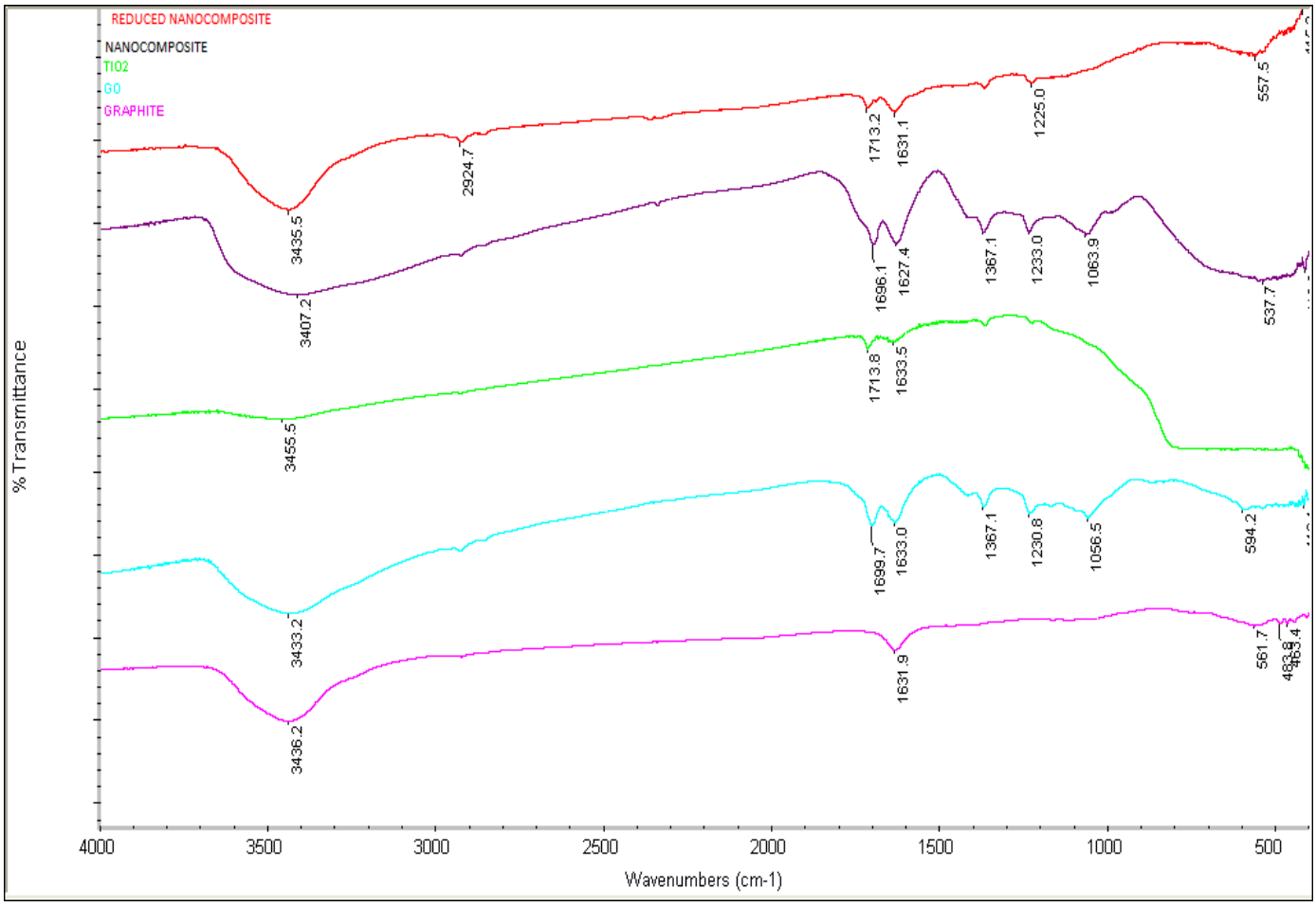

Fig 11: FTIR spectra of graphite, GO, TiO_2, GO-TiO_2 nanocomposite and Reduced GO-TiO_2 nanocomposite

Fig 11 shows the FTIR spectra of **graphite, GO, TiO_2, GO-TiO_2 nanocomposite and reduced GO-TiO_2 nanocomposite.** A prominent adsorption peak appeared at 3407 cm^{-1} reveals to the stretching vibrations of the hydroxyl (O-H) group present in GO. This -OH bond may be due to the presence of alcoholic, phenolic, carboxylic and so on. Because of presence of water at this vibrational frequency it also confirms the hydrophilic properties of prepared GO. Further, the peaks at 1696, 1233 and 1064 cm^{-1} give the stretching vibrations of carbonyl group (C=O), the epoxide groups and alkoxy group. The C=C stretching is present at the band of 1627 cm^{-1} which gives the signature of unoxidised carbon groups. The spectra also showed strong absorption band at 538 cm^{-1}, indicating the presence of Ti-O-Ti bond in TiO_2. With regard the presence of different oxygen containing functional groups, it can be verified that synthesized GO is highly hydrophilic in nature.

4.2 UV-vis spectroscopy

Fig 12 shows UV-vis spectra of graphite, graphene, titanium oxide and graphene oxide and titanium dioxide nanocomposite. It can be seen that GO-TiO_2 naocomposite shows strong absorbance at wavelength 230 nm where as TiO_2 shows absorbance over a range of wavelength 350 to 550 nm.

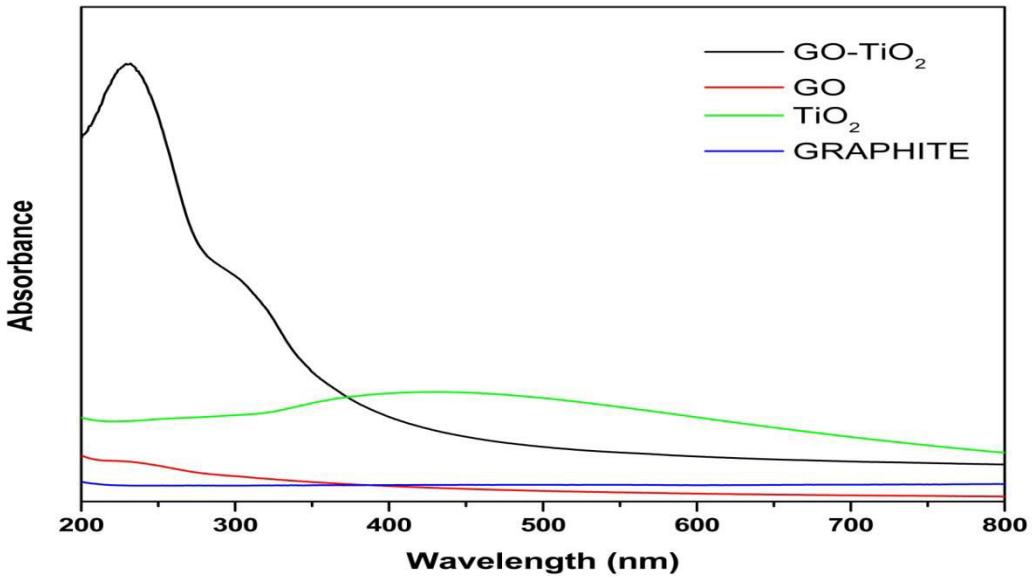

Fig 12: UV-vis specta of Graphite, GO, TiO_2 and GO-TiO_2 nanocomposite

4.3 POWDER X-RAY DIFFRACTION ANALYSIS

X-ray diffraction is an analytical tool used for the identification of the atomic and molecular structure of crystals, in which the incident ray gets diffracted into many directions. By observing the intensities and the angles of the diffracted beam we can give a 3-D picture of the electron density in the crystal and hence by using this information we can determine the various chemical bonds, a disorder in the crystal and much other information like the plane of the crystal, interlayer distance between the planes. In our present work, we have done the XRD of the synthesized GO and GO-TiO_2 nanocomposite, and a comparison is done with the pristine graphite. XRD spectra is measured in the range of 2Θ from 10° to 50°, which show a diffraction peak of pristine graphite at an angle of 26° and d which is distance between the layers is calculated by using Brags equation, i.e. ,2d SinΘ=nλ, ---------- (4)

Which is nearly equal to 3.34Å for graphite. As the oxygen functionalities group introduced to the graphite, there is an expansion of the graphite layers and the interlayer spacing increases in the graphite, and hence the diffraction angle should be less. It is clearly observed in the XRD spectra of GO (fig 13) the diffraction angle for GO is at an angle of 12° and hence the interlayer spacing of the stacks is nearly equal to 7.97 Å.

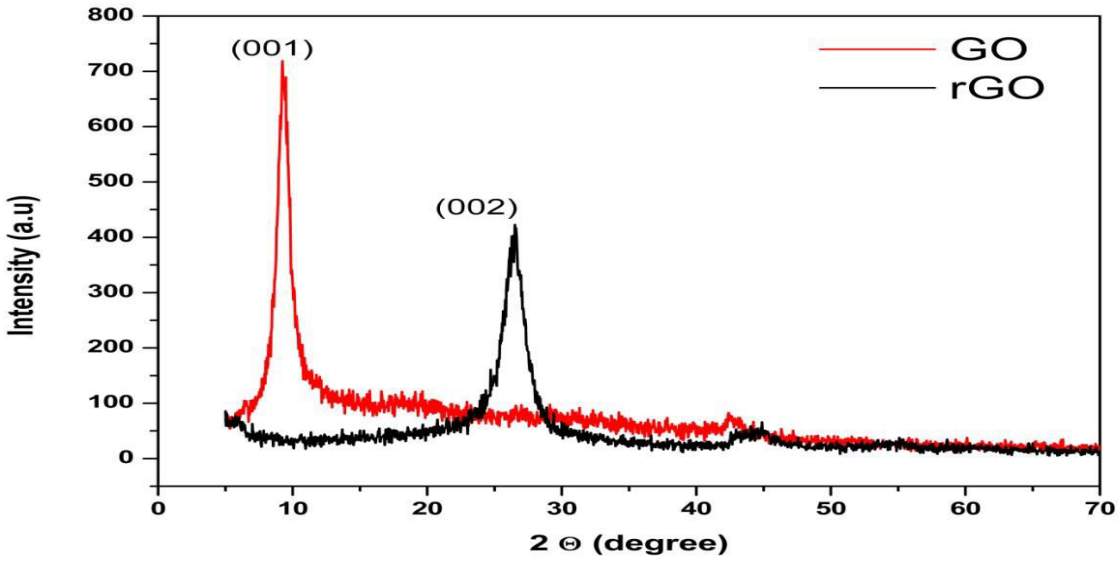

Fig 13: XRD pattern of graphite and graphene oxide (GO)

Fig 14 shows the XRD pattern of GO-TiO_2 nanocomposite. GO-TiO_2 nanocomposite shows sharp peaks at $2\Theta = 10^o$, 25^o, 38^o, 54^o, 56^o and 63^o corresponds to (001), (110), (101), (211), (221), (220) and (310) respectively.

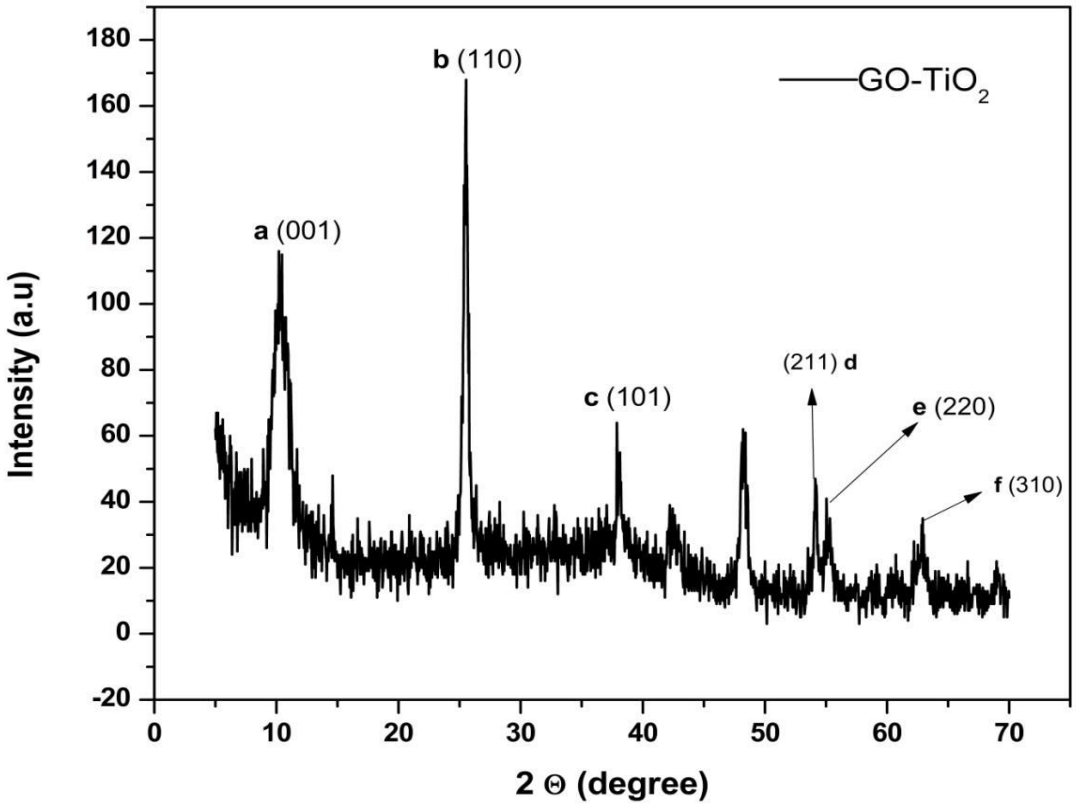

Fig 14: XRD pattern of GO-TiO_2 nanocomposite

4.4 DIFFERENTIAL SCANNING CALORIMETRY

Fig 15 shows the DSC thermogram which indicates the trace of GO-TiO_2 nanocomposite. It can be seen that the nanocomposite shows strong peak in endothermic region, which shows the melting point of nanocomposite, i.e. , 225 ^oC.

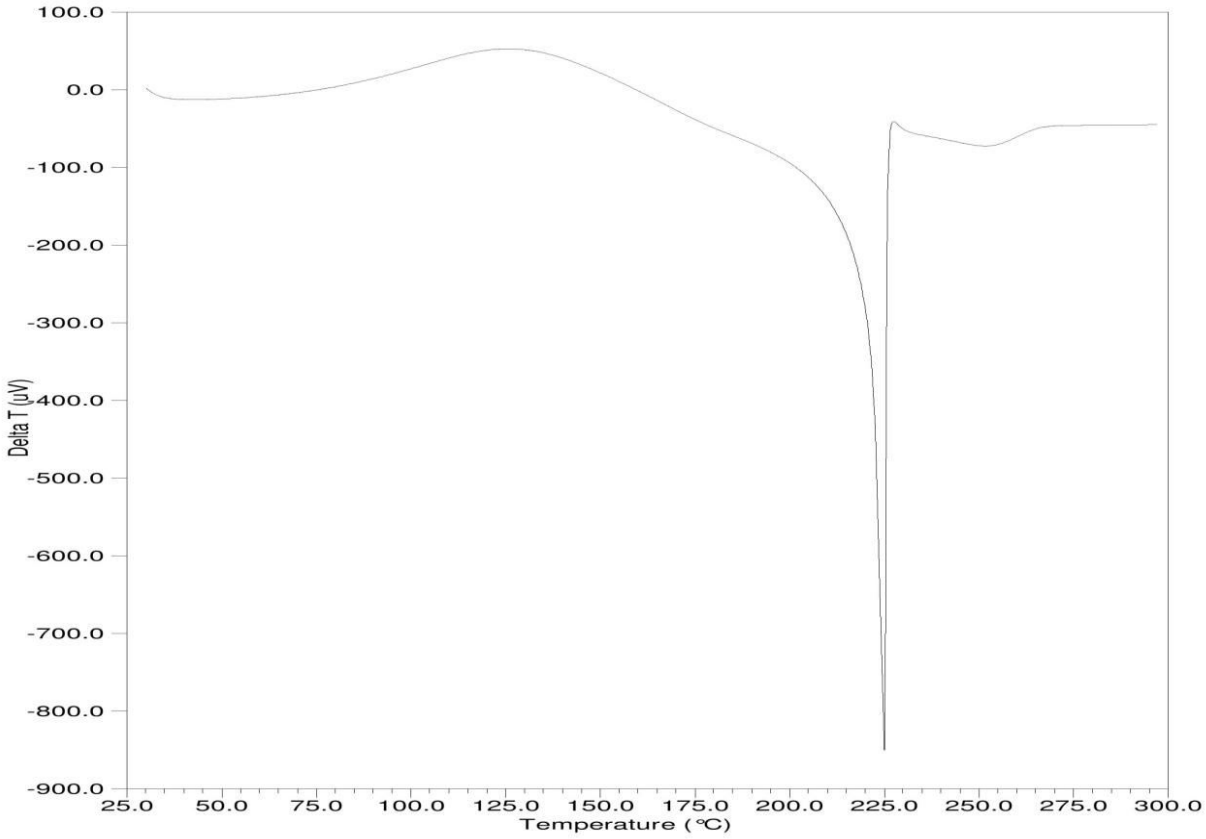

Fig 15: DSC analysis of GO-TiO_2 nanocomposite

4.5 CYCLIC VOLTAMMETRY STUDIES

Cyclic voltammetry (CV) is a type of potentiodynamic electrochemical measurement techniques. In CV, the working electrode potential is ramped linearly against time. Unlike in linear sweep voltammetry, when the set potential is reached in a CV experiment, the working electrode's potential is ramped in the opposite direction so that it would return to its initial potential. These cycles of ramps in potential may be repeated as many times as needed. The pictorial view of Potentiostat/Galvanostat by Autolab is shown in fig 16.

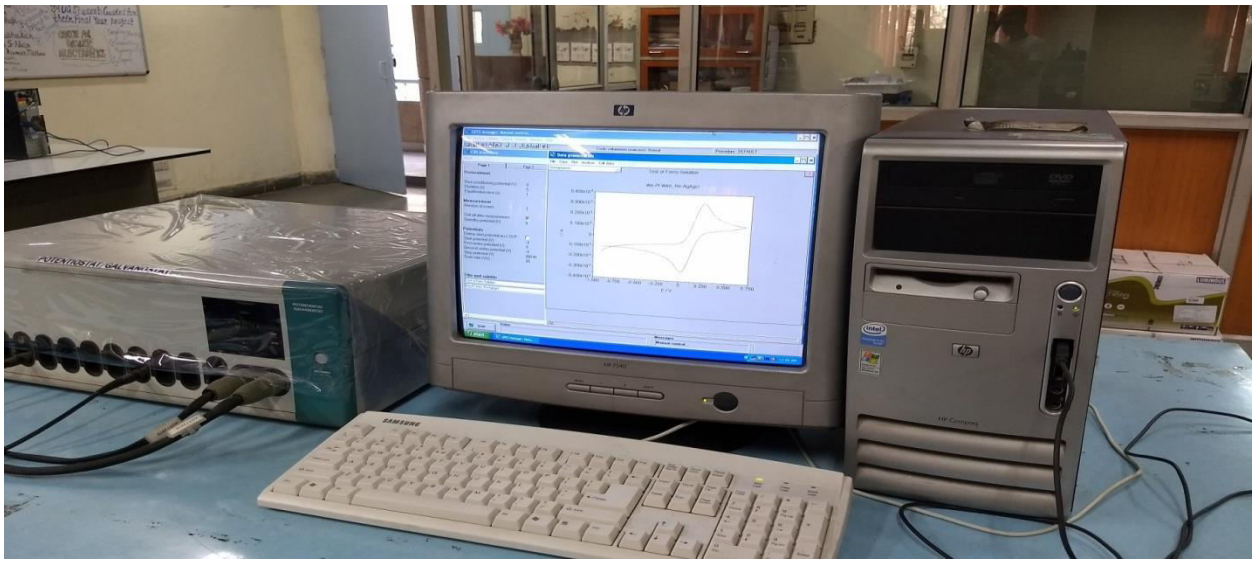

Fig 16: Pictorial view of Potentiostat/Galvanostat by Autolab

The current at the working electrode is plotted versus the applied voltage (that is, the working electrode's potential) to get the cyclic voltammogram trace as shown in fig 17. CV is done to study the electrochemical properties of an analyte in solution [41,42].

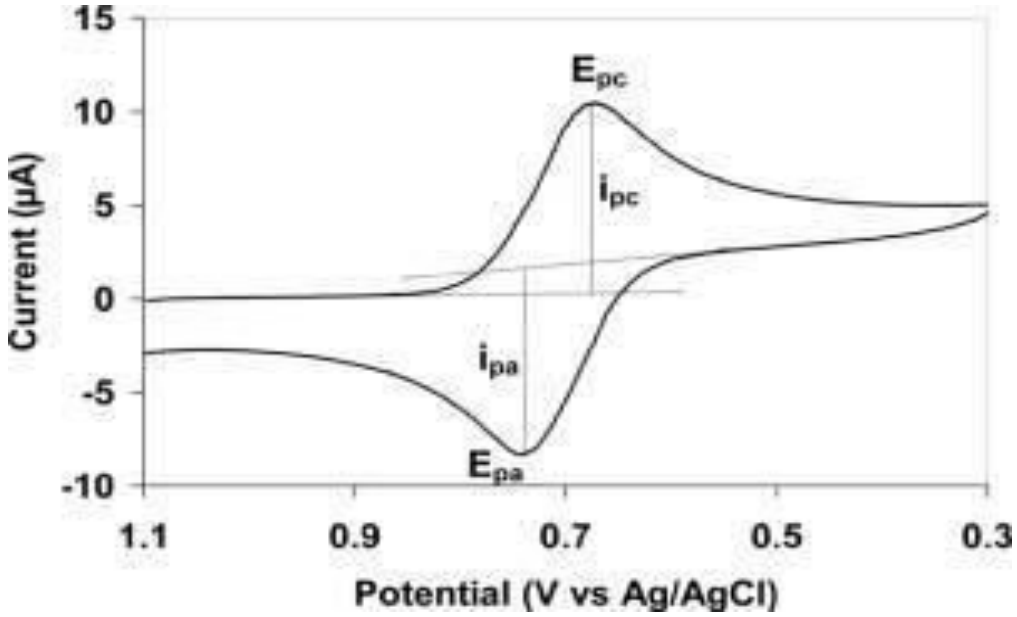

Fig 17: Typical cyclic voltammogram where i_{pc} and i_{pa} show the peak cathodic and anodic current respectively for a reversible reaction.

Fig 18 shows the three electrode system used for cyclic voltammetry analysis . Fig 19 shows the deposited films of GO-TiO_2 nanocomposite over ITO coated glass on which CV tests are performed.

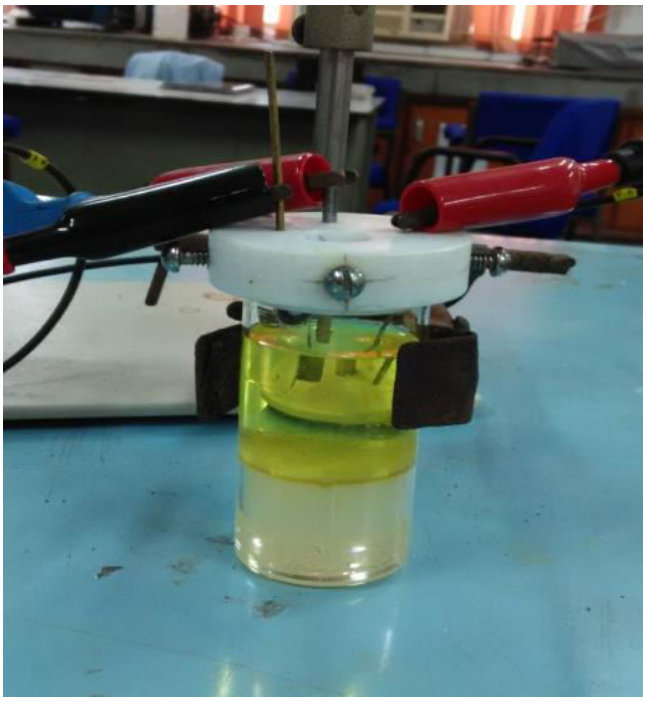

Fig 18: Three electrode system for CV

Fig 19: Deposited film of nanocomposite over ITO coated glass

Table 2 shows the kinetic parameters for fabricated bioelectrode, i.e. , GO-TiO_2/ITO. The GO shows increase in electron transfer coefficient as compared to ITO. There is about two-fold increment in electron transfer coefficient in case of GO-TiO_2 nanocomposite (α = 0.75) as compared to TiO_2 (α = 0.31) but little bit lower than GO. There is an increase in diffusion coefficient for GO-TiO_2 nanocomposite when deposited at 12 V (D = 6.10809×10^{-14}) as compared to GO and GO-TiO_2 nanocomposite when deposited at 15 V.

Table 2: Kinetic parameters calculated for fabricated electrode

S. No	Name of the electrode	Electron transfer coefficient ,α	Average surface coverage, Ґ/ mol cm^{-2}	Diffusion coefficient, D/cm^2s^{-1}
1.	ITO	0.508	9.6949×10^{-14}	0.57697×10^{-13}
2.	TiO_2	0.31	4.253×10^{-11}	1.1546×10^{-13}
3.	GO_12V	0.975	2.7925×10^{-12}	1.58156×10^{-16}
4.	GO-TiO_2_12 V	0.752	4.8247×10^{-11}	6.10809×10^{-14}
5.	GO-TiO2_15V	0.753	2.760×10^{-11}	1.998×10^{-14}

The results of CV studies obtained as a function of scan rate (10–300 mV s^{-1}) for the GO-TiO_2 /ITO electrode which is shown in fig 20 & 21. The positive and negative peaks correspond to the oxidation and reduction reactions of the $[Fe(CN)_6]^{3-/4-}$ redox pair, respectively.

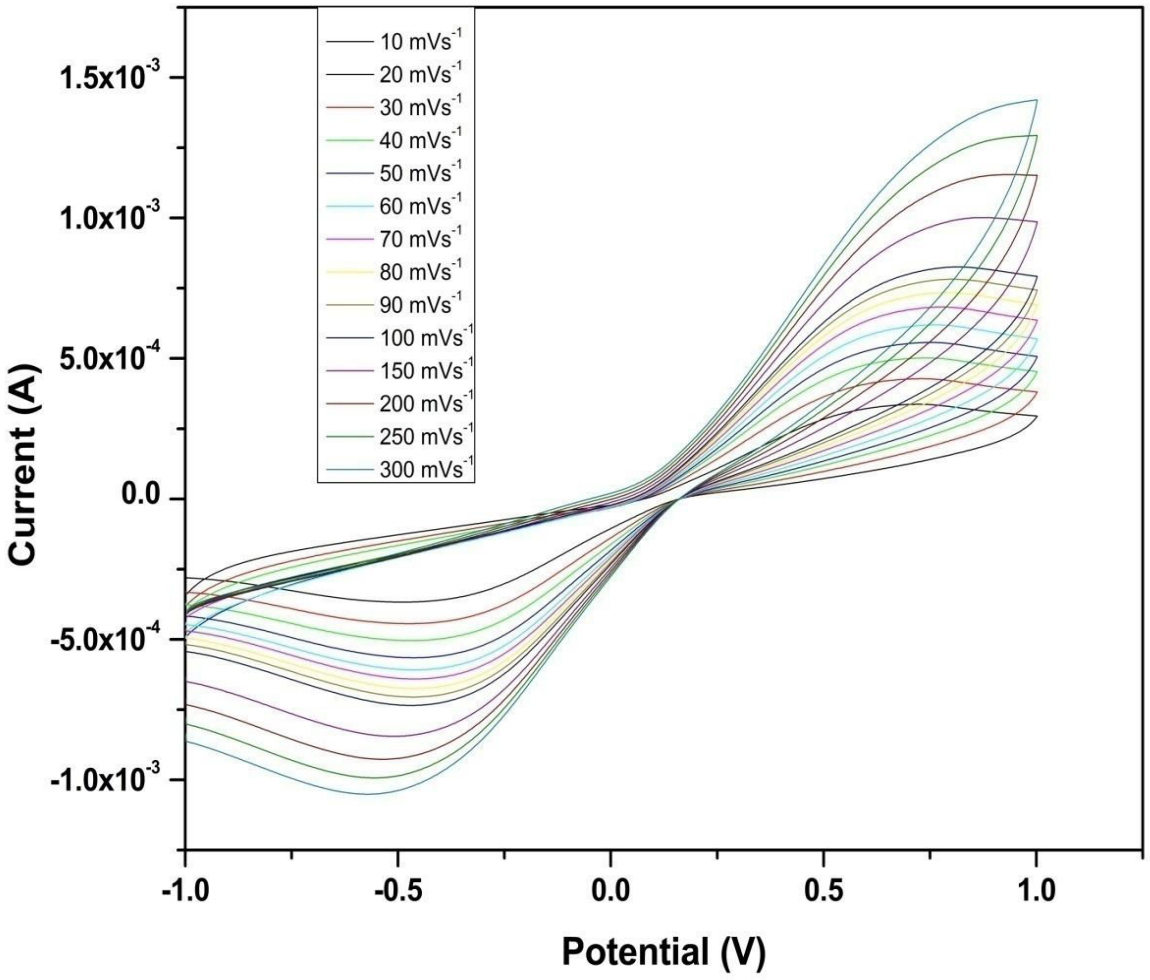

Fig 20: Cyclic voltammogram (CV) of GO-TiO_2 (film deposited at 12 V)/ITO

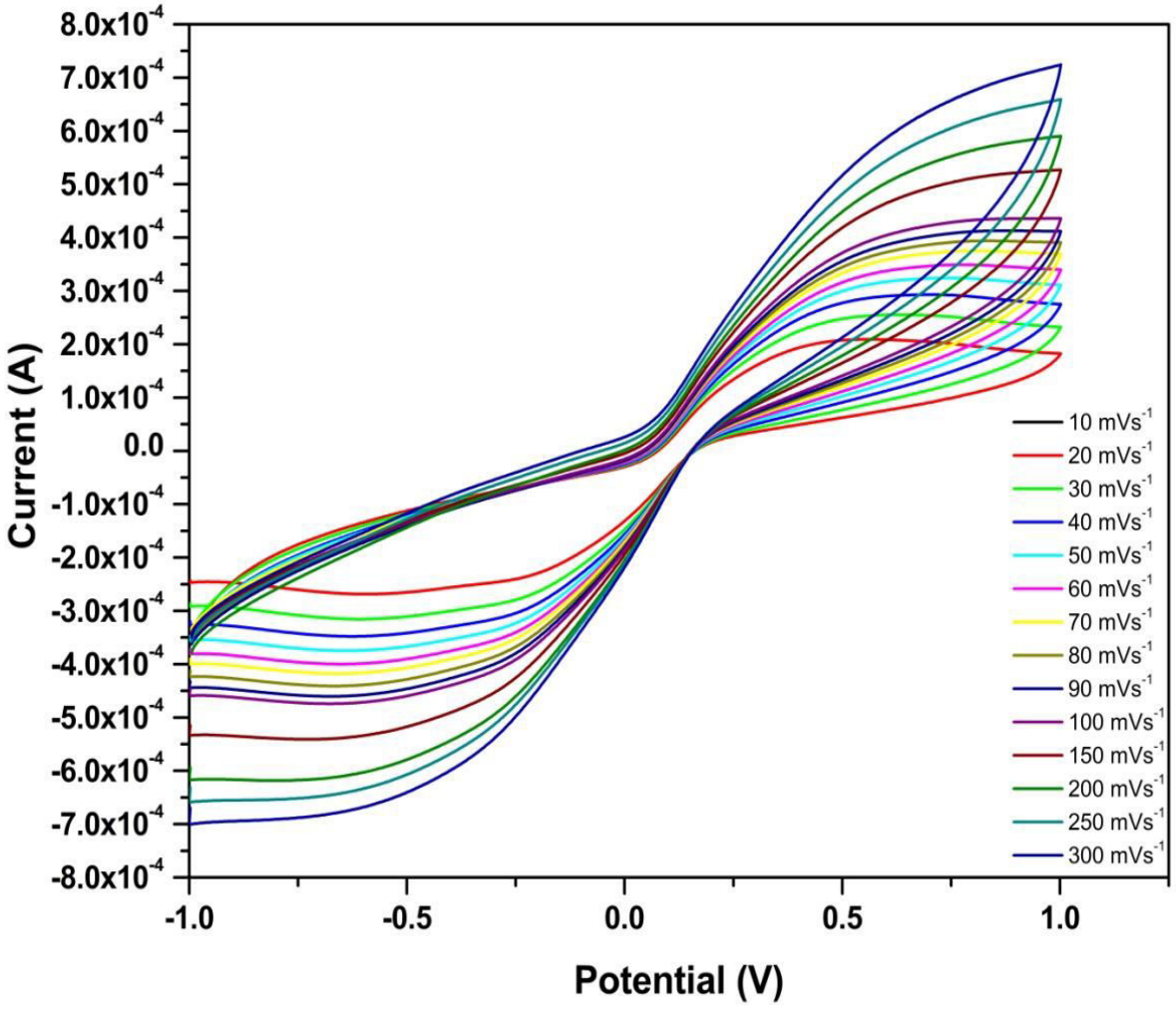

Fig 21: Cyclic voltammogram (CV) of GO-TiO_2 (film deposited at 15 V)/ITO

The peak currents I_p for both oxidation and reduction follow a linear relation with respect to the square root of scan rate indicating the existence of diffusion-controlled electrochemical reaction rates for the redox pair at the electrode. It can be seen that the oxidation peak shifts to a more positive value and the reduction peak to more negative values with the increase of the scan rate and both the peak potentials are linearly dependent on the log of the scan rate, which agrees well with Laviron's theory and may be given as:

$E_{pa} = E_o + X \ln[(1 - \alpha)Fv/RTk_s]$

$E_{pc} = E_o + Y \ln[(\alpha)Fy/RTk_s]$ - (2)

$\mathbf{lnk_s = \alpha \ln(1 - \alpha) + (1 - \alpha)\ln \alpha - \ln(RT/nFy) - \alpha (1 - \alpha)nFDE_p/RT}$ - (3)

Where α and k_s are the electron transfer coefficient and charge transfer rate constant, respectively.

The plot of ln y versus the anodic peak potential (E_{pa}) and cathodic peak potential (E_{pc}) yields two straight lines with their slopes of **X = RT/(1 -** α**)nF** and**Y = RT/** α **nF**, respectively. Based on the plot the values of α and k_s have been determined.

According to Laviron's equation, the relationship between peak current (I_p) and surface coverage can be described as:

$\mathbf{I_p = n^2F^2vA\ G\ (4RT)^{-1}}$ - (4)

Where, I_p is peak current, n is the number of electrons transferred, v is the scan rate (50 mV s^{-1}), A is the electrode area (0.25 cm^2), and G is the average surface coverage of the electrode redox substance (mol cm^{-2}).

Taking the average of both the cathodic and anodic results, G is found. On the basis of the linear slope of the anodic peak currents on the square root of the potential sweep rates, and the Randles-Sevcik equation,

$\mathbf{I_p = (2.99 * 10^5)\ \alpha^{1/2} n^{3/2} ACD^{1/2} v^{1/2}}$ - (5)

Here n is the number of transferred electron for the redox reaction, C is the molar concentration of $[Fe(CN)6]^{3-/4-}$, and v is the scan rate (50 mV s^{-1}). By performing a linear regression for I_p versus $v^{1/2}$, the slope S can be obtained and the effective surface area of the electrode (A) is calculated to

$$A = S/ (2.99 * 10^5)\, n^{3/2}\, \alpha^{1/2} C D^{1/2} \quad \text{- (6)}$$

Fig 22 shows the cyclic voltammogram of GO, GO-TiO_2 (deposited at 12 and 15V), TiO_2, ITO at scan rate 30 mVs^{-1}.The GO-TiO_2 (deposited at 12 V) shows highest anodic peak current, i.e. , 4.277×10^{-4} A.

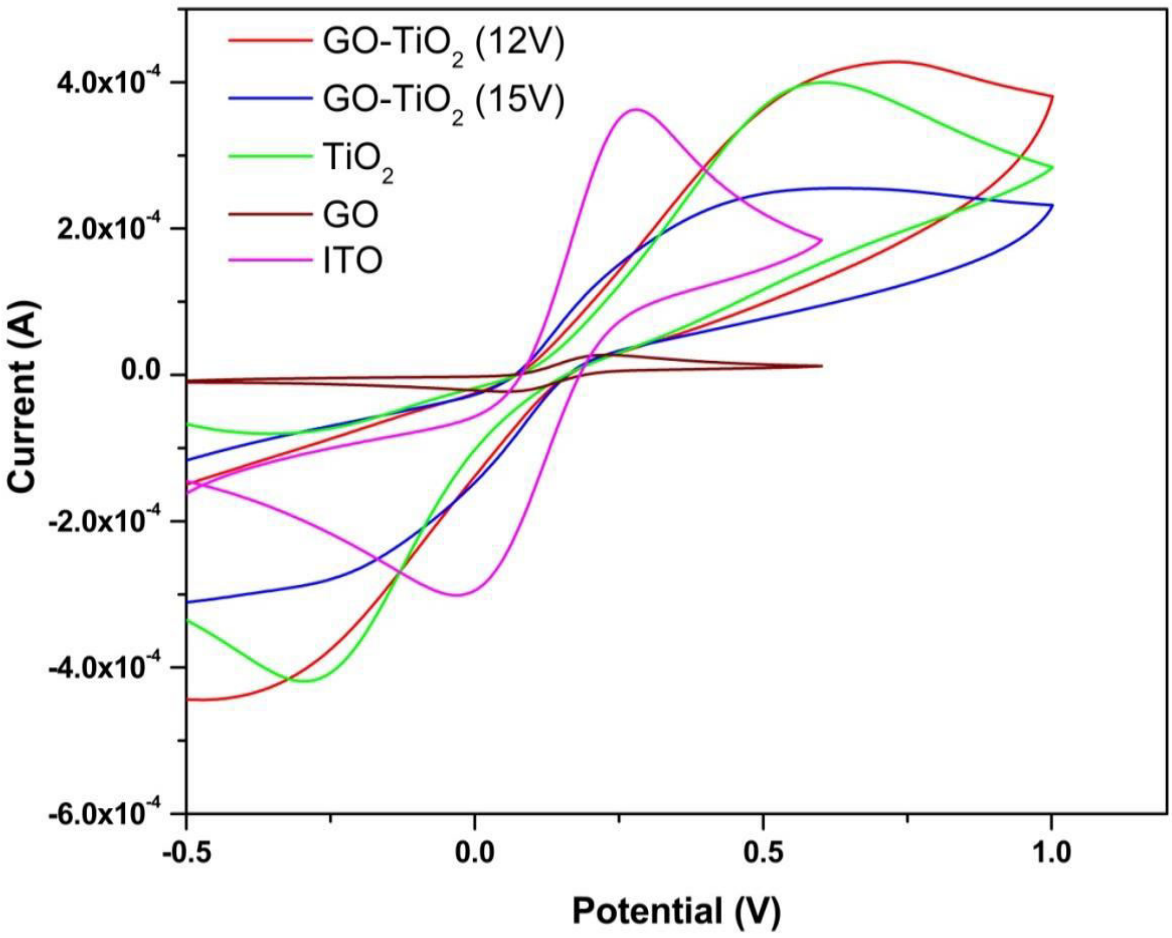

Fig 22: Cyclic voltammogram of GO, GO-TiO_2 (deposited at 12 and 15V), TiO_2, ITO at scan rate 30 mVs^{-1}

The results of CV studies obtained as a function of scan rate (10–250 mV s^{-1}) for the GO /ITO electrode which is shown in fig 23. The positive and negative peaks correspond to the oxidation and reduction reactions of the $[Fe(CN)_6]^{3-/4-}$ redox pair, respectively.

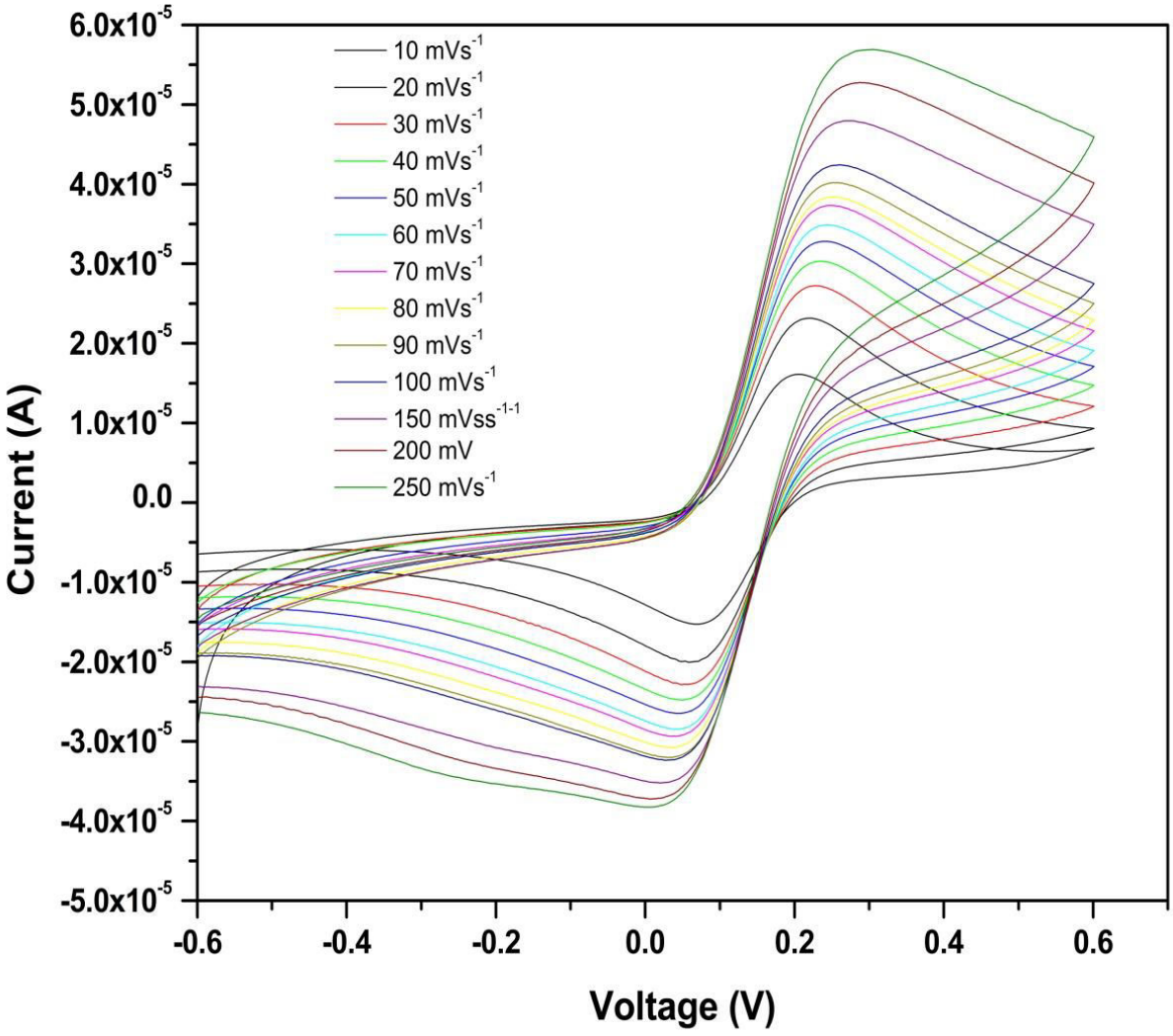

Fig 23: Cyclic voltammogram (CV) of Graphene Oxide (GO)/ITO

The results of CV studies obtained as a function of scan rate (10–300 mV s^{-1}) for the TiO_2 /ITO electrode which is shown in fig 24. The positive and negative peaks correspond to the oxidation and reduction reactions of the $[Fe(CN)_6]^{3-/4-}$ redox pair, respectively.

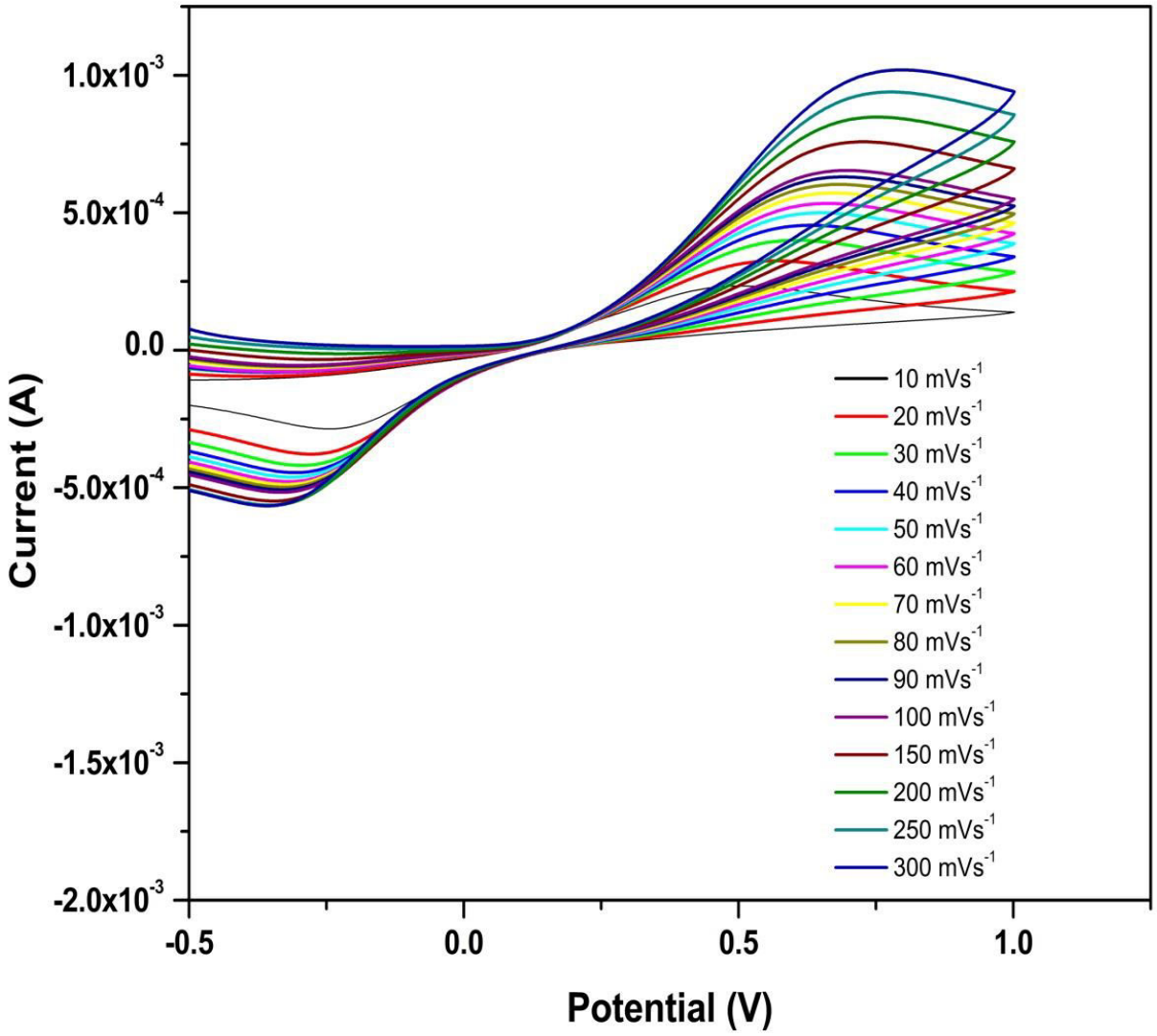

Fig 24: Cyclic voltammogram (CV) of TiO_2/ITO

The results of CV studies obtained as a function of scan rate (10–300 mV s^{-1}) for the ITO electrode which is shown in fig 25. The positive and negative peaks correspond to the oxidation and reduction reactions of the $[Fe(CN)_6]^{3-/4-}$ redox pair, respectively.

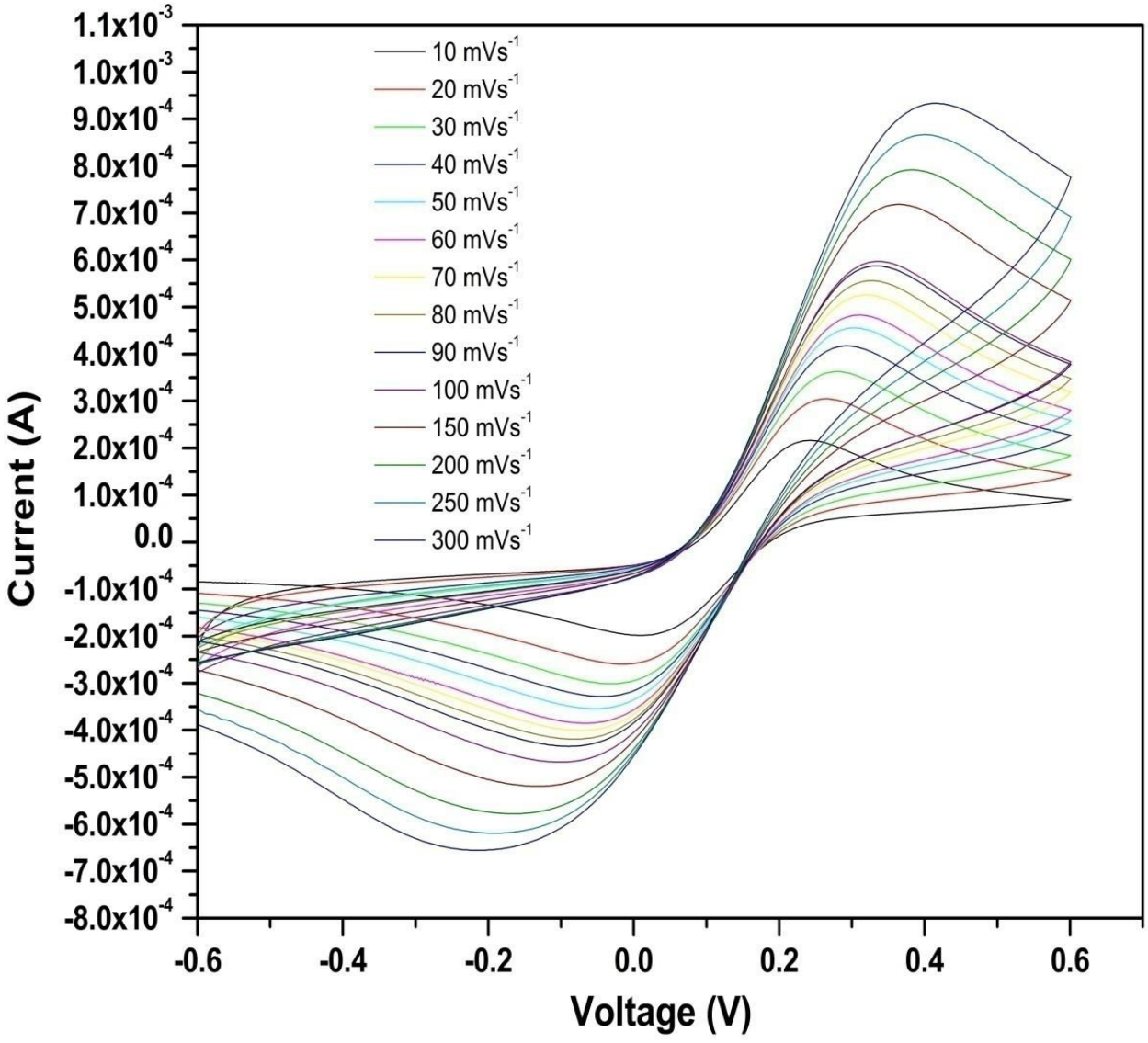

Fig 25: Cyclic voltammogram (CV) of ITO

4.6 SCANNING ELECTRON MICROSCOPY

SEM was used to study the surface morphology of the TiO_2 and GO-TiO_2 nanocomposite. Fig 26(a) shows the SEM micrograph of TiO_2 nanoparticles at 10 μm. It shows the nearly spherical and uniformly distributed of the TiO_2 nanoparticles. The fig 26 (b) shows the SEM micrograph of GO-TiO_2 nanocomposites taken at 5 μm. It clearly shows the change in appearance of TiO_2 due to formation of nanocomposites with graphene oxide (GO). Highly agglomerated particles with very small size, uniformly distributed and nearly spherical morphology can be seen easily in nanocomposites.

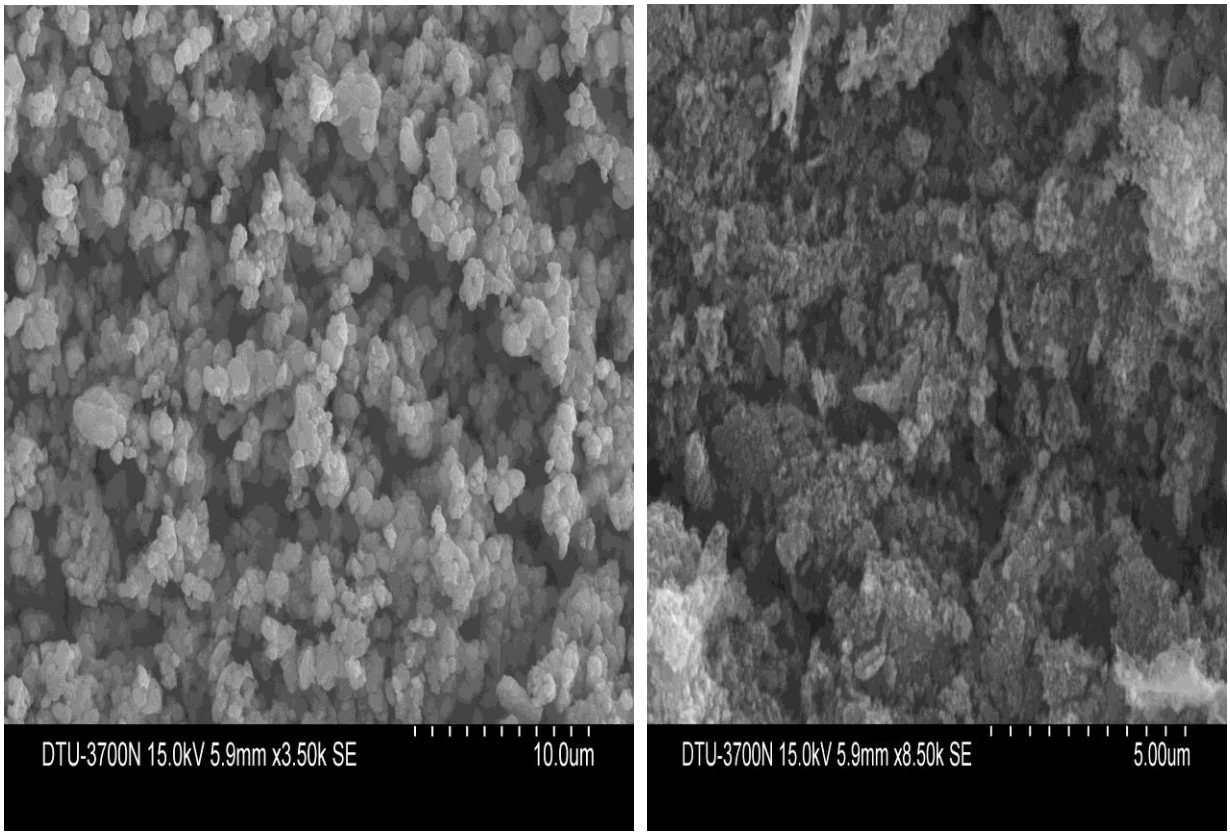

(a) (b)

Fig 26: SEM micrograph (a) TiO_2 nanoparticles (b) GO-TiO_2 nanocomposites

4.7 HYDROGEN PEROXIDE (H_2O_2) SENSING

4.7.1 Why Hydrogen Peroxide sensing is required?

- Hydrogen peroxide (H_2O_2) is a very simple compound in nature but with great importance in pharmaceutical, clinical, environmental, mining, textile and food manufacturing applications.
- H_2O_2 can also be used as a signalling molecule in regulating diverse biological processes such as immune cell activation, vascular remodelling, apoptosis, stomatal closure and root growth in living organisms
- H_2O_2 is also a side product generated from some classic biochemical reactions catalyzed by enzymes such as glucose oxidase (GOx), alcohol oxidase (AlOx), lactate oxidase (LOx), urate oxidase (UOx), cholesterol oxidase (ChoOx), glutamate oxidase (GlOx), lysine oxidase (LyOx), oxalate oxidase (OxaOx), etc.
- Electrochemistry may offer easy, fast, responsive, and cost effective means as H_2O_2 is an electroactive molecule [28] in comparison of other conventional techniques.

Fig 27 shows Electrochemical response of the H_2O_2/GO-TiO_2/ITO bioelectrode obtained as a function of H_2O_2 concentration from 50 to 200 μM using cyclic voltametry. The anodic peak current corresponds to the H_2O_2 concentration, i.e. ,100 mM in PBS (pH 7.4) containing 5 mM $[Fe(CN)_6]^{3-/4-}$ is 8.15×10^{-3} mA increases to 3.84×10^{-2} mA corresponds to 200 μM H_2O_2 concentration μM in PBS (pH 7.4) containing 5 mM $[Fe(CN)_6]^{3-/4-}$ as shown in fig 28.

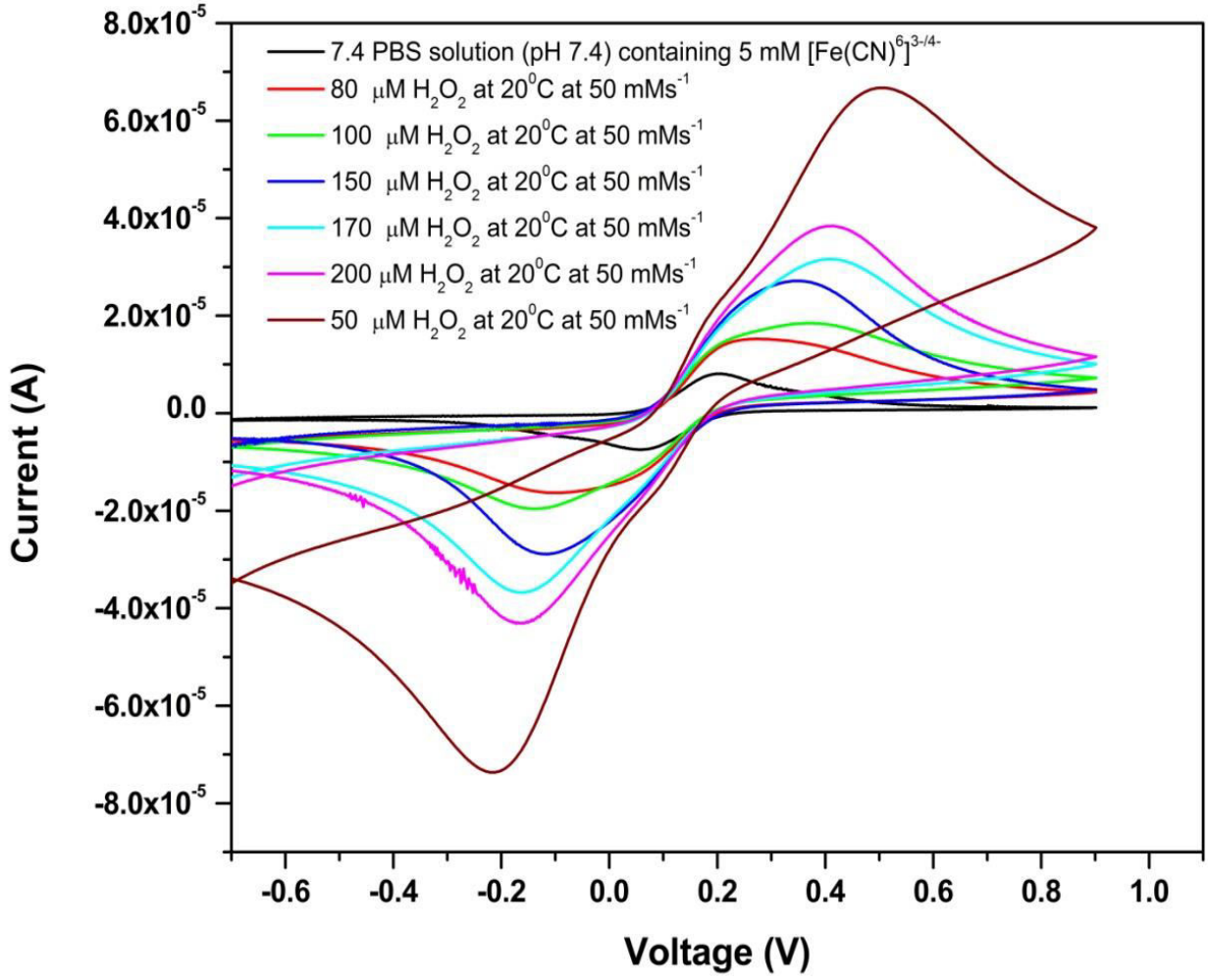

Fig 27: Electrochemical response of the H_2O_2/GO-TiO_2/ITO bioelectrode obtained as a function of H_2O_2 concentration (50 µM to 200 µM) using CV

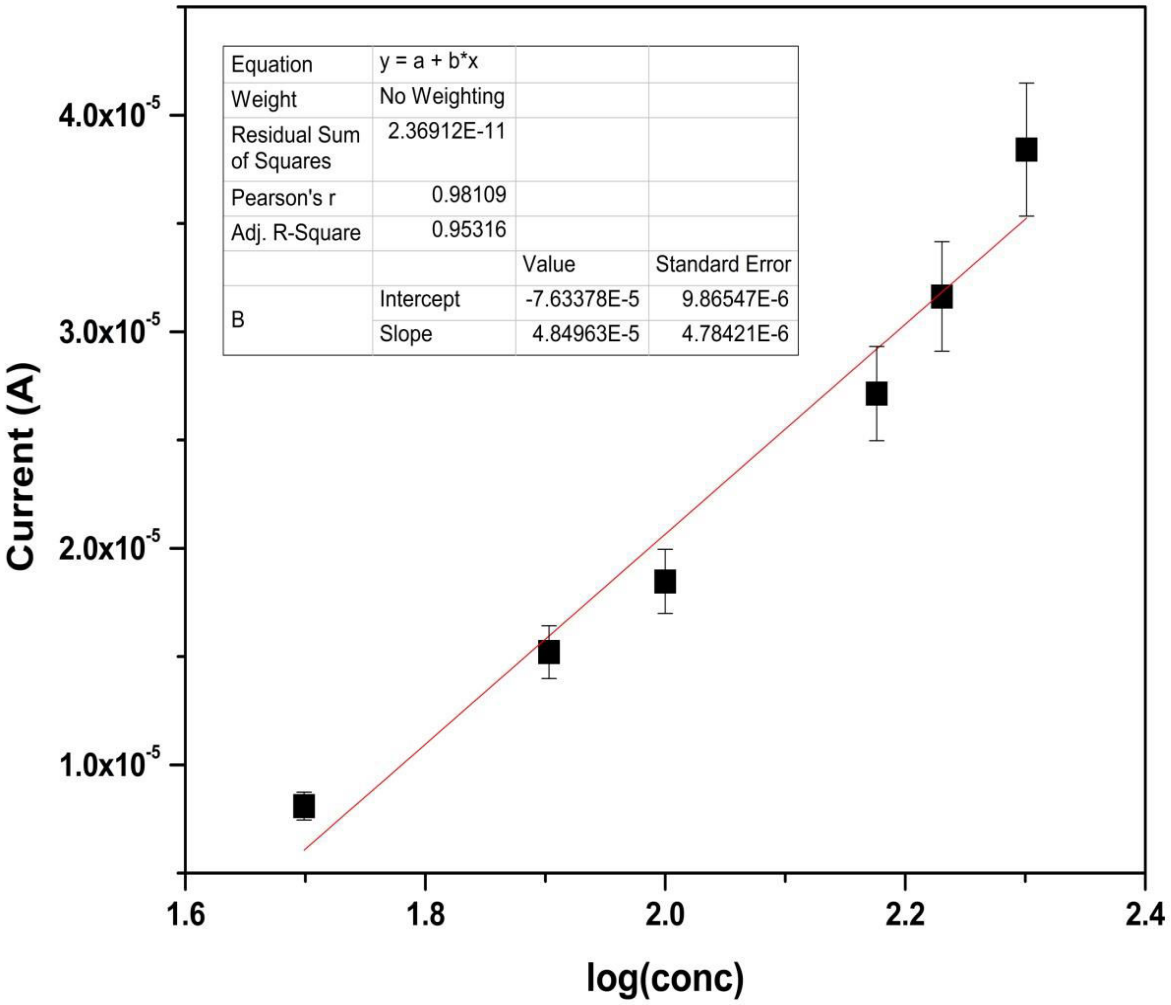

Fig 28: Calibration plot between the anodic peak current and H_2O_2 concentrations

CHAPTER 5

CONCLUSIONS

Graphene oxide and graphene oxide – Titanium dioxide nanocomposite have been successfully synthesized at optimized conditions. Electron microscopy and XRD clearly reveals the successful formation of GO and GO-TiO_2 nanocomposite whereas FTIR studies suggest its functionalized nature. A well dispersed GO solution and GO-TiO_2 in distilled water has been utilized for the electrophoretic deposition (EPD) of GO and its nanocomposite onto ITO electrode using Mg $(NO_3)_2.6H_2O$ as an electrolyte. Electrochemical studies show that there is an increase in the value of average surface coverage and diffusion coefficient in case of GO-TiO_2 film as compared to GO film on ITO. The electrochemical sensing studies of the hydrogen peroxide shows increase in anodic peak current with increase in H_2O_2 concentration in PBS (pH 7.4) containing 5 mM $[Fe(CN)_6]^{3-/4-}$.

REFERENCES

[1] A.K. Geim, A.H. MacDonald, Phys. Today 60 (2007) 35.

[2] H. Chen, M.B. Müller, K.J. Gilmore, G.G. Wallace, D. Li, Adv. Mater. 20 (2008) 3557.

[3] S. Stankovich, D.A. Dikin, G.H.B. Dommett, K.M. Kohlhaas, E.J. Zimney, E.A. Stach, R.D. Piner, S.T. Nguyen, R.S. Ruoff, Nature 442 (2006) 282.

[4] S. Gilje, S. Han, M.S. Wang, K.L. Wang, R.B. Kaner, Nano Lett. 7 (2007) 3394.

[5] J.S. Bunch, Z.A.M. Vander, S.S. Verbridge, I.W. Frank, D.M. Tanenbaum, J.M. Parpia, H.G. Craighead, P.L. McEuenh, Science 315 (2007) 490.

[6] J.B. Wu, H.A. Becerril, Z.A. Bao, Z.F. Liu, Y.S. Chen, P. Peter, Appl. Phys. Lett. 92 (2008) 263302.

[7] C.S. Shan, H.F. Yang, J.F. Song, D.X. Han, A. Ivaska, L. Niu, Anal. Chem. 81 (2009) 2378.

[8] Y. Wang, Y.M. Li, L.H. Tang, J. Lu, J.H. Li, Electrochem. Commun. 11 (2009) 889.

[9] X.L. Luo, J.J. Xu, W. Zhao, H.Y. Chen, Biosens. Bioelectron. 19 (2004) 1295.

[10] X. Cui, G. Liu, Y. Lin, J. Biomed. Nanotechnol. 1 (2005) 1.

[11] X.B. Lu, J.H. Zhou, W. Lu, Q. Liu, J.H. Li, Biosens. Bioelectron. 23 (2008) 1236.

[12] X.H. Shu, Y. Chen, H.Y. Yuan, S.F. Gao, D. Xiao, Anal. Chem. 79 (2007) 3695.

[13] N.V. Klassen, D. Marchington, H.C.E. McGovan, Anal. Chem. 66 (1994) 2921.

[14] M.C.Y. Chang, A. Pralle, E.Y. Isacoff, C.J. Chang, J. Am. Chem. Soc. 126 (2004) 15392.

[15] C. Matsubara, N. Kawamoto, K. Takamura, Analyst 117 (1992) 1781.

[16] D.W. King, W.J. Cooper, S.A. Rusak, B.M. Peake, J.J. Kiddle, D.W. O'Sullivan, M.L. Melamed, C.R. Morgan, S.M. Theberge, Anal. Chem. 79 (2007) 4169.

[17] J.B. Jia, B.Q. Wang, A.G. Wu, G.J. Cheng, Z. Li, S.J. Dong, Anal. Chem. 74 (2002) 2217.

[18] X.L. Luo, J.J. Xu, Q. Zhang, G.J. Yang, H.Y. Chen, Biosens. Bioelectron. 21 (2005) 190.

[19] B. Wang, J.J. Zhang, Z.Y. Pan, X.Q. Tao, H.S. Wang, Biosens. Bioelectron. 24 (2009)1141.

[20] C. G. Tsiafoulis, P. N. Trikalitis and M. I. Prodromidis, Electrochem. Commun., 7(2005) 1398.

[21] M. Geiszt and T. L. Leto, J. Biol. Chem. 279 (2004) 51715.

[22] M. Giorgio, M. Trinei, E. Migliaccio and P. G. Pelicci, Nat. Rev. Mol. Cell Biol., 8 (2007), 722.

[23] C. Laloi, K. Apel and A. Danon, Curr. Opin. Plant Biol., 7 (2004) 323.

[24] J. H. Lee, I. N. Tang and J. B. Weinstein-Lloyd, Anal. Chem., 62 (1990) 2381.

[25] S. Hanaoka, Anal. Chim. Acta, 426 (2001) 57.

[26] E. Fernandes, A. Gomes and J. L. F. C. Lima, J. Biochem. Biophys. Methods, 65 (2005) 45.

[27] M. C. O. R. F. P. Nogueira and W. C. Paterlini, Talanta, 66 (2005) 86.

[28] J. Wang, Biosens. Bioelectron.,21 (2006) 1887.

[29] W. Zhang, G.F. Wang, X.J. Zhang, B. Fang, Electroanalysis 21 (2009) 179.

[30] J. Pillay, K.I. Ozoemena, Electrochim. Acta 54 (2009) 5053.

[31] Salimia, R.G. Comptonb, R. Hallaja, Anal. Biochem. 333 (2004) 49.

[32] J.J. Gooding, R. Wibowo, J.Q. Liu, W.R. Yang, D. Losic, S. Orbons, F.J. Mearns, J.G. Shapter, D.B. Hibbert, J. Am. Chem. Soc. 125 (2003) 9006.

[33] J. Wang, Electroanalysis 17 (2005) 7.

[34] H.H. Kuh,et al. "Towards real application of conducting materials" , Synthetic Metals, 71 (2139) 1995.

[35] D.R. Dreyer et al. "From Conception of Realization: An Historical Account of Graphene and Some Perspectives for its Future", Angew Chem. Int. Ed 49 (2010) 9336.

[36] Y. Zhu et al. "Graphene and Graphene Oxide: Synthesis, Properies and Applications" Adv. Mater. 22 (2010) 3906.

[37] A.T. Collins, "The Optical and Electronic Properties of Semiconducting Diamond". Phil. Trans. Royal Soc. A, 342 (1993) 233.

[38] Fullerene encyclopedia britanica.

[39] M.F.L. De Volder, "Carbon Nanotubes: Present and Future Commercial Applications", science, 39 (2013) 535.

[40] S.Iijima, "Carbon nanotubes: past, present and future". Phys B.; 1 (2002) 323.

[41] Bard, Allen J.; Larry R. Faulkner. *Electrochemical Methods: Fundamentals and Applications* (2 ed.). Wiley. ISBN 0-471-04372-9, 12 (2000) 18.

[42] Nicholson, R. S.; Irving. Shain. "Theory of Stationary Electrode Polarography. Single Scan and Cyclic Methods Applied to Reversible, Irreversible, and Kinetic Systems.". *Analytical Chemistry*. 01 (1964) 04.